

In vitro cell migration quantification method for scratch assays

Ana Victoria Ponce Bobadilla^{*1,2}, Jazmine Arévalo³, Eduard Sarro³, Helen M Byrne⁴, Philip K Maini⁴, Thomas Carraro^{1,2}, Simone Balocco^{5,6}, Anna Meseguer^{3,7,8}, and Tomás Alarcón^{†9,10,11,12}

¹ Institute for Applied Mathematics, Heidelberg University, 69120 Heidelberg, Germany

²Interdisciplinary Center for Scientific Computing (IWR), Heidelberg University, 69120 Heidelberg, Germany

³Renal Physiopathology Group, CIBBIM-Nanomedicine, Vall d’Hebron Research Institute, Barcelona, Spain

⁴Wolfson Centre for Mathematical Biology, Mathematical Institute, University of Oxford, Oxford OX2 6GG, UK

⁵Dept. Matemàtics and Informàtics, University of Barcelona, Gran Via 585, 08007 Barcelona, Spain

⁶Computer Vision Center, 08193 Bellaterra, Spain

⁷ Departament de Bioquímica i Biologia Molecular, Unitat de Bioquímica de Medicina, Universitat Autònoma de Barcelona, Bellaterra; Spain

⁸ Red de Investigación Renal (REDINREN), Instituto Carlos III-FEDER, Madrid, Spain

⁹ ICREA, Pg. Lluís Companys 23, 08010 Barcelona, Spain

¹⁰ Centre de Recerca Matemàtica, Edifici C, Campus de Bellaterra, 08193 Bellaterra (Barcelona), Spain

¹¹Departament de Matemàtiques, Universitat Autònoma de Barcelona, 08193 Bellaterra (Barcelona), Spain

¹² Barcelona Graduate School of Mathematics (BGSMath), Barcelona, Spain

Abstract

The scratch assay is an in vitro technique used to assess the contribution of molecular and cellular mechanisms to cell migration. The assay can also be used to evaluate therapeutic compounds before clinical use. Current quantification methods of scratch assays deal poorly with irregular cell-free areas and crooked leading edges which are features typically present in the experimental data. We introduce a new migration quantification method, called “monolayer edge velocimetry”, that permits analysis of low quality experimental data and better statistical classification of migration rates than standard quantification methods. The new method relies on quantifying the horizontal component of the cell monolayer velocity across the leading edge. By performing a classification test on in silico data, we show that the method exhibits significantly lower statistical errors than standard methods. When applied to in vitro data, our method outperforms standard methods by detecting differences in the migration rates between different cell groups that the other methods could not detect. Application of this new method will enable quantification of migration rates from in vitro scratch assay data that cannot be analysed using existing methods.

Keywords— scratch assays, migration quantification methods, migration rates

1 Background

Cell migration plays a fundamental role in developing and maintaining the organization of multicellular organisms, while aberrant cell migration is found in many pathological disorders like cancer and atherosclerosis [1, 2]. Cell migration involves the movement of individual cells, cell sheets, or cell clusters from one location to another [3]. Two main types of migration can be distinguished: single cell migration and collective cell migration. During collective cell migration multiple cells perform a coordinated movement regulated by cell-cell adhesion, collective cell polarization, coordination of cytoskeletal activity and chemical and mechanical cues [1]. In vitro assays are central to the study of cell migration since they allow us to quantify cell migratory capacity under controlled experimental conditions [3, 4]. The scratch or wound healing assay is the method of choice for studying cell migration due to the low cost and simplicity of its experimental design [4, 5]. A scratch assay involves: growing a cell monolayer to confluence in a multiwell assay plate; creating a “wound” -a cell-free zone

^{*}anavictoria.ponce@iwr.uni-heidelberg.de

[†]Talarcon@crm.cat

in the monolayer- into which cells can migrate; and monitoring the recolonisation of the scratched region to quantify the cell migration [5] (see Figure 1). This experimental technique is commonly used to understand the molecular mechanisms that affect cell migration [6, 7] and to identify pharmaceutical compounds that can modulate cell migration and consequently drive treatment therapies [8]. Given the key role of scratch assays in biomedical research, it is important to develop robust quantification methods that accurately measure and compare migration rates of different scratch assays.

Multiple quantification methods are used to assess collective cell migration in scratch assays [9]. The most common ones focus on wound width or area change [3, 10]. Such methods use a number of metrics to quantify migration, including the percentage difference in the wound width at different time points [7, 11], wound width at specific time points [12], and the slope of a linear approximation to the change in wound area [13], among others. Other more computationally intensive methods exist that rely on cell tracking or on determining a velocity field across the full monolayer [14, 15]. In this work we focus on less computationally intensive methods that permit a quick assessment of collective cell migration. A weakness of the aforementioned methods is that they do not perform well when the two borders of the scratch are not perfectly straight, a feature which is common in experimental data [13, 16]. The lack of a reproducible wounding procedure results in non-uniform cell-free areas with irregular leading edges, as can be seen in Figure 1. Furthermore, migration rate measurements have been shown to be sensitive to the initial degree of confluence [17] and the initial geometry of the wound [18]. Current quantification methods require high quality experimental data which are difficult to obtain; therefore, frequently the experimental data are discarded or need to be produced again.

Another issue with existing quantification methods is that many of them use time-specific measurements to determine differences in migration rates of cell samples. Typically, a time point in the course of the experiment is considered at which the wound area or width of each sample is measured. Then, statistical tests are performed on these measurements with the purpose of detecting significant differences [3]. The time points of comparison are not standardized and vary across studies [7, 19, 20]. Differences in the time points used for comparison may be due to differences in the proliferation rates of the cell types under consideration. The choices are made to minimize the impact of cell proliferation on migration quantification. However, there is no standard procedure for choosing the comparison time even though the choice can affect the comparison and may render the results from the analysis unreliable.

In this work, we introduce a new quantification method that tackles these issues and can be used to analyse lower quality experimental data. Irregular leading edges are accounted for by approximating the front by a piecewise constant function, which is constant over windows with a fixed size, w^* . We assume that within each window, the contour moves with constant speed in the perpendicular direction until the left and right leading edges meet. The migration in the scratch assay is characterized by a series of linear approximations to the interface’s position over time in these windows.

The paper is organized as follows: in Section 2.1 we describe our experimental system and in Section 2.2 we present the agent-based model that we use to simulate the in vitro process. In Section 2.4 we introduce the new migration quantification method for scratch assays and describe the two quantification methods to which we compare it: the *percentage wound area method*, which is widely used, and the *closure rate method*, reviewed in [13]. In Section 3.1.1, we investigate how the velocity distribution, determined by our quantification method, is affected by cell migration and proliferation. In Section 3.1.2 we show that the method correctly classifies cells with different migration and proliferation parameters. In Section 3.1.3 we show the statistical comparison against the other methods. In Section 3.2.3 we present the results of applying the three methods to an experimental data set. Finally in Section 4, we discuss our results and present our conclusions.

2 System and methods

2.1 Cell culture and wound healing assay

Six site-specific mutations in a latent transcription factor that regulates downstream genes involved in essential biological processes, including migration, were generated. Mutants S1, S2, S3, S4, S5 and S6 were then transduced into a human renal carcinoma cell line, 769-P (ATCC CRL-1933), through lentiviral particles. The 769-P mutants were cultured in Dulbecco’s Modified Eagle’s Medium (DMEM) (#42430, Gibco) supplemented

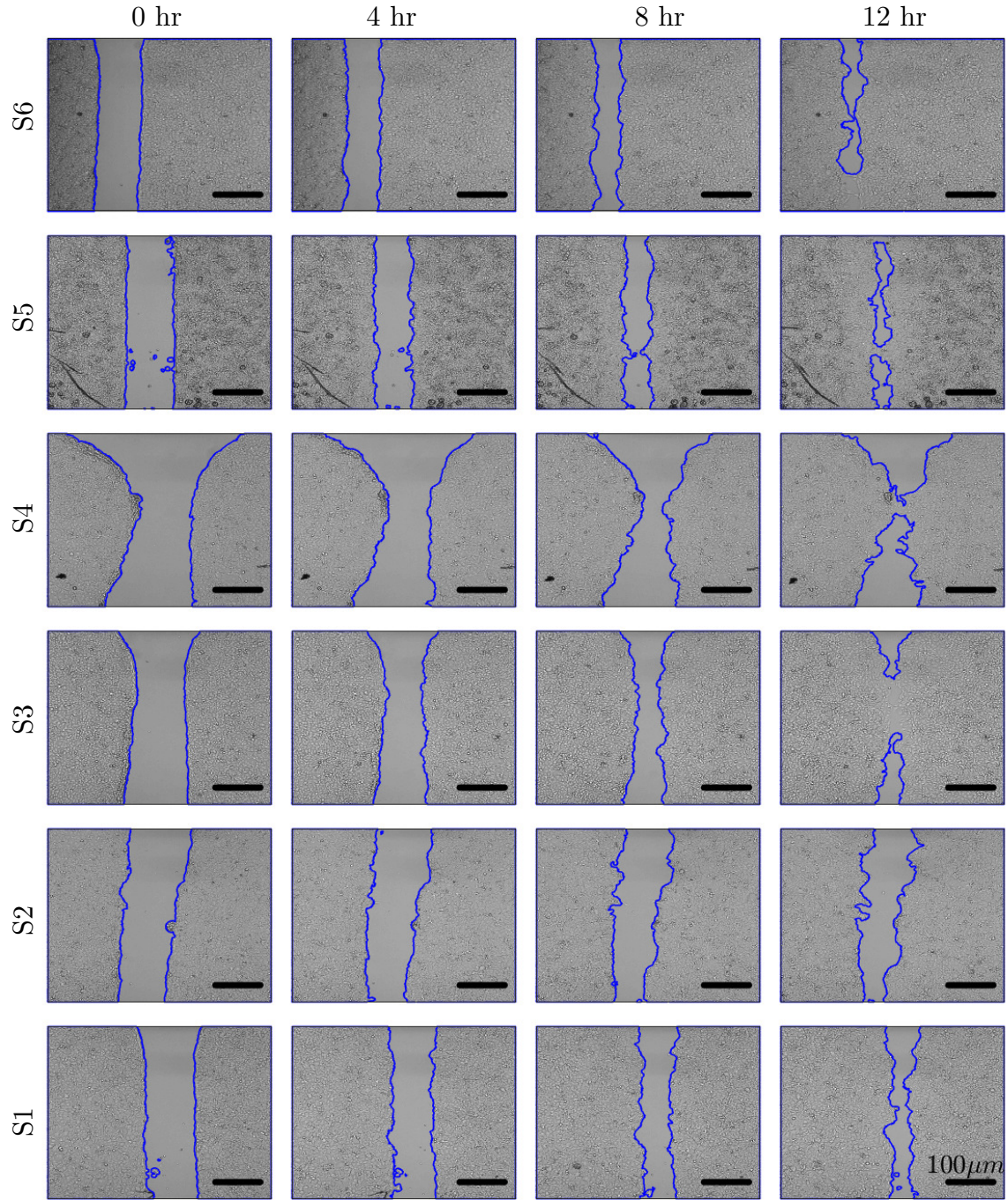


Figure 1: Time-lapse images of a representative scratch assay from each of the six experimental cell groups (S1-S6) are plotted at time 0 hr, 4 hr, 8 hr and 12 hr. In each image, the leading edges were detected by applying the segmentation algorithm. The resulting interfaces/cell fronts are plotted in blue.

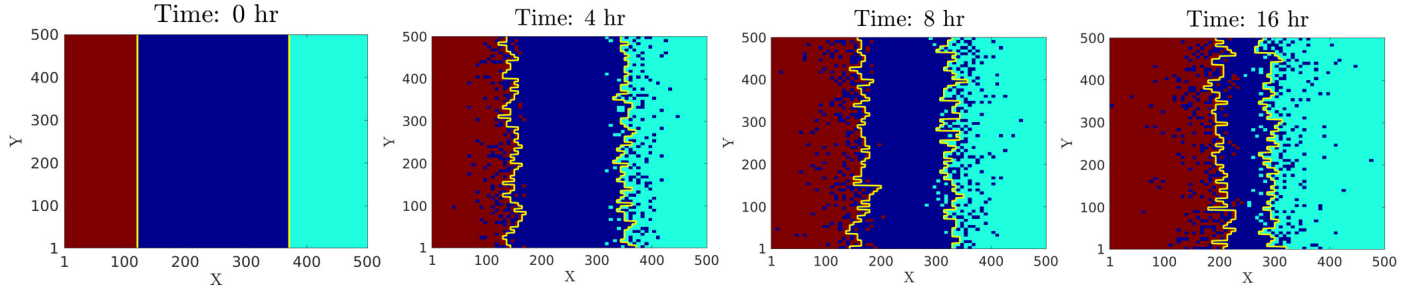


Figure 2: Evolution of an agent-based simulation. We considered an idealised initial condition and fixed the migration and proliferation parameters so that $p_m = 0.3$ and $p_p = 0.01$, respectively. The recolonisation of the wounded region is shown at times $t = 0, 4, 8$ and 16 hr. For ease of visualisation, the two cell monolayers (right and left) are plotted with different colours (red and turquoise), while the area devoid of cells is coloured blue. The leading edges detected by the segmentation algorithm are plotted in yellow.

with 10% of fetal bovine serum (FBS) (#10270, Gibco), 1% of sodium pyruvate solution 100 mM (#03-042-1B, Biological Industries) and 1% of antibiotic-antimycotic solution 100X (#15240, Gibco). Cells were maintained at 37°C in 5% CO_2 .

For the wound healing assay, the 769-P mutants (S1-S6) were seeded at 0.025×10^6 cells per well in a 2 well silicone insert with a defined cell-free gap (Ibidi #81176, Germany), incubated and allowed to grow for 48 hr. Once the cells reached 100% confluence, the culture insert was removed and the area that remained clear of cells was quantified for 24 hr using the Live Cell-R Station (Olympus). Digital images were obtained every 30 minutes.

Data consisted of 24 wound healing assays: four replicates for each of the six groups (S1-S6). Each assay consisted of 48 images. The imaged region size was $500 \times 500 [\mu\text{m}]^2$.

2.2 Agent-based model of the scratch assay

We consider an agent-based model that has been previously used to simulate in vitro cell cultures [21, 22, 23]. The simulation domain is a two-dimensional square lattice, with the same dimensions as the experimental images: $[0, D] \times [0, D]$ where $D = 500 \mu\text{m}$. The lattice spacing, Δ , which is interpreted as the average cell diameter, is set to $10 \mu\text{m}$ unless otherwise specified.

In this model each agent can either proliferate or move within the simulation domain. We consider an end time of $T = 24$ hr and an update time of $\tau = 0.1$ hr. We include crowding effects by assuming that each lattice site is occupied by at most one cell. A cell with centre at (x, y) is said to be at (x, y) . Zero flux boundary conditions are imposed. At each update time, agents move and/or proliferate with migration and proliferation probabilities p_m and p_p , respectively. Since typical estimates of the cell doubling time are approximately 15-30 h [24, 25], whereas the time required for a cell to move a distance equal to its diameter is of the order of 10 min [26], we consider migration and proliferation probabilities in the ranges $p_m \in [0, 1]$ and $p_p \in [0, 0.01]$, respectively. The simulation algorithm and typical parameter values are presented in the Supplementary Material Section S1. In Figure 2 we plot the evolution of a typical realisation of the agent-based model for which the migration and proliferation parameters are given by $p_m = 0.3$ and $p_p = 0.01$.

2.3 Automatic contour segmentation

The leading edges of the cell monolayers from the experimental images are detected by applying a segmentation algorithm based on the Growcut method [27]. The method is a robust technique, already employed in several computer vision applications, that performs a binary image segmentation.

The Growcut algorithm requires the initial specification of a subset of pixels from each type of region: cell monolayer and unoccupied space; these pixels are referred to as *seeds*. The seeds should be located far from the leading edges, where all the pixels of such an area belong to one of the two classes. The algorithm evolves as follows: at each iteration, the pixels surrounding the initial seeds are assigned to one class or the other,

adjusting the size of each region. The classification depends on the similarity of the pixel intensity with respect to the pixel intensity of the seeds.

In our implementation, the seeds are chosen as follows: for the cell region, the Canny and Roberts edge contour methods [28, 29] are used to select the pixels with the highest variability, corresponding to the cell contours. For the background region, the seeds are set in areas having a low variability, defined as areas in which the pixel intensity has a standard deviation less than 500.

After applying the detection algorithm to each image, we have a record of the positions of the left and the right interfaces at each time where the image was taken. At each vertical position, the interface is considered to be the closest pixel to the wound.

2.4 Migration quantification methods

We first introduce the two established quantification methods for scratch assays. Then, we introduce a new method that quantifies the x-component of the velocity of the leading edge of the cell monolayer.

2.4.1 Area method

One of the most widely used quantification methods, which we term the *area method*, assesses the migration in an indirect manner. During an experiment, the wound area percentage, $\hat{A}(t)$, is tracked:

$$\hat{A}(t) := \frac{A(t)}{A(0)} \times 100\%$$

where $A(t)$ is the wound area at time t and $A(0)$ is its initial area. The migration rate is then indirectly evaluated as the percentage wound area at a specific time point.

2.4.2 Closure rate method

In [13] cell migration is quantified by assuming that the wound area reduces linearly over time. We refer to this method as the *closure rate method*. The change in wound area $A(t)$ is first approximated by a linear function:

$$A(t) \approx m \times t + b \quad (1)$$

where m and b are real scalars. The wound area is assumed to be the length of the field-of-view (l) times the width of the gap ($W(t)$). Since l is constant during the course of the experiment, Equation (1) becomes:

$$\frac{dA}{dt} \approx l \times \frac{dW}{dt}. \quad (2)$$

The migration rate, C_r , is defined to be half of the width closure rate

$$C_r := \frac{1}{2} \frac{dW}{dt}. \quad (3)$$

Combining Equations (2) and (3), we have

$$C_r = \frac{|m|}{2 \times l}. \quad (4)$$

2.5 Proposed quantification method: Monolayer edge velocimetry (MEV)

We propose a new strategy for quantifying front migration in a scratch assay using a set of representative velocities. We denote by t_0, \dots, t_N , the times at which data are collected. Let $X \times Y$ represent the square domain of the processed image, $X = Y = \{1, \dots, D\}$ where D is the number of pixels. For each $j \in Y = \{1, \dots, D\}$, we denote the interface position in the horizontal direction, at the j -th vertical position and at time point t_n , as $i_j(t_n)$ where $1 \leq i_j \leq D$. See Figure 3 (a) for a schematic representation.

To determine the velocities, we assume a linear approximation to the front position over time for a window size w . The linear approximation is determined in two steps:

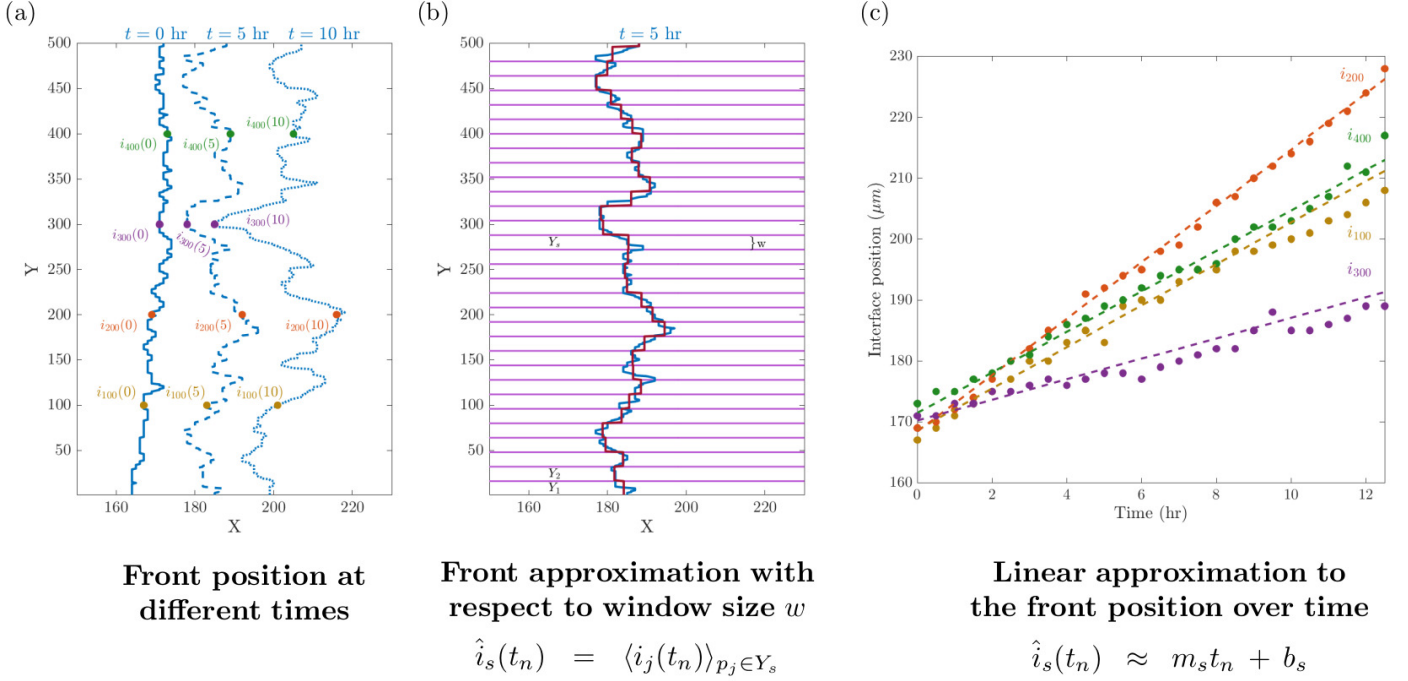


Figure 3: Linear approximation of the front position over time with respect to window size w for one of the scratch assays from the experimental cell groups. (a) To introduce the notation, the positions of the left front at times $t = 0, 5$ and 10 hr are plotted in blue. The solid line corresponds to $t = 0$ hr; the dashed line to 5 hr and the dotted line to 10 hr. The front positions at the $100, 200, 300$ and 400 y-coordinates for these times are plotted: yellow, orange, purple and green, respectively. (b) The left front at $t = 5$ hr is approximated by a window size w . Y is partitioned into M segments denoted Y_s , $1 \leq s \leq M$, each with length w . A magenta horizontal line delimits each segment. The front position is plotted in blue and the approximated front position, taken as an average over each Y_s , is plotted in red. (c) The time evolution of the interfaces at the $100, 200, 300$ and 400 y-coordinates and the linear approximation with respect to the window size $w = 16$ are plotted using dotted lines and dashed lines, respectively. The window size $w = 16$ is the window size that maximizes the objective function (7).

1. First, the front position is approximated for the window size, w . Y is divided into $M = D/w$ segments denoted Y_s , $1 \leq s \leq M$, each of length w . The front position \hat{i}_s in each segment Y_s is approximated by its mean position,

$$\hat{i}_s(t_n) = \langle i_j(t_n) \rangle_{i_j \in Y_s}. \quad (5)$$

This procedure is illustrated in Figure 3 (b).

2. The dynamics of the front position in each window is approximated by linear regression, so that

$$\hat{i}_s(t_n) \approx m_s t_n + b_s. \quad (6)$$

In Figure 3 (c) the dotted lines indicates how the actual front position changes over time at selected y-coordinates; the dashed lines represent the corresponding linear approximations for a window of size $w = 16$.

By performing this approximation for the left and right interfaces, we obtain a set of velocities $\{|m_s|\}_{s=1}^{2M}$ to which we refer as the windowed velocities for window size w .

A necessary step in our method is determining the window size to perform the linear approximation (6). We observe that as the window size decreases, the fitness of the linear approximation improves. This observation prompts us to consider the smallest window size, however, for window sizes smaller than the average cell size, the left and right windowed velocity distributions are significantly different. This is a finite size sampling effect, since the scale on which the velocities are quantified is much smaller than the cell size scale. Therefore the individual velocity of each cell at the front is counted multiple times and its value is over represented, producing a bias in the overall windowed velocity distribution. To deal with the finite size sampling effect, we choose a window size for which the left and right windowed velocity distributions are similar. We note that if two different cell types are seeded on either side then the assumption of left and right similarity can no longer be made. However, in the standard experimental setup of the scratch assay, the left and right interfaces are from the same cell type. A more detailed explanation of why the similarity of the left and right velocity distributions should be considered is included in Section S2.1 of the Supplementary Material.

We use two criteria to select the optimal window size, w^* : (i) fitness of the approximation, and (ii) similarity of the left and right windowed velocity distributions. In more detail, we introduce an objective function, $F(w)$, that has three terms and enables us to find the optimal window size with respect to these two criteria:

$$F(w) = Fit_{resid}(w) + Fit_{Rsquared}(w) + Fit_{KS_{distance}}(w). \quad (7)$$

- $Fit_{resid}(w)$ measures the discrepancy between the interface position over time and the linear approximation (Equation (6)).
- $Fit_{Rsquared}(w)$ considers the coefficient of determination, R^2 , which describes how well the interface position's variance over time is explained by the linear approximation [30].
- $Fit_{KS_{distance}}(w)$ is a distance function derived from the Kolmogorov-Smirnov statistic for the two-sample Kolmogorov-Smirnov (K-S) test [30]; it calculates the distance between the left and right front windowed velocity distributions.

These terms are scaled such that the window size that maximises the objective function takes into account the trade-off between giving the best fit and having the left and right velocity distributions closest to each other.

The procedure used to determine the optimal window size can be interpreted as a procedure that optimizes the number of velocities needed to characterize the migration. Detailed information about how to modify the objective function when multiple assays are considered can be found in Supplementary Material Section S2.

The procedure used to determine the set of representative velocities is summarized in Algorithm 1.

Algorithm 1 : Monolayer edge velocimetry

- 1: Determination of the optimal window size for the linear approximation using the objective function (7)

$$w^* = \max_{1 \leq w \leq D} F(w) \quad (8)$$

where $F(w)$ is given by equation (7).

- 2: Linear approximation, with respect to the window size w^* ; indicating how the positions of the left and right interfaces change over time,

$$\hat{i}_s(t_n) \approx m_s t_n + b_s$$

where $\hat{i}_s(t_n) = \langle i_j(t_n) \rangle_{i_j \in Y_s}$, $Y = \bigcup_{s=1}^M Y_s$ in which $|Y_s| = w^*$ and $M = D/w^*$.

Output: $\{|m_s|\}_{s=1}^{2M}$ is the representative set of velocities that quantify cell migration in the scratch assay.

We refer to the “Monolayer edge velocimetry method” as the MEV method in the rest of the paper.

2.6 Classification test

In order to assess the performance of the three quantification methods in a controlled way, we use the agent-based model to generate *in silico* scratch assays. In particular, we compare the ability of the different methods to distinguish between cell populations with different proliferation and migration parameters. We consider the following classification test:

1. We fix a focal parameter combination $\hat{P} = (p_{\hat{m}}, p_{\hat{p}}) \in [0, 1] \times [0, 0.01]$ and run n simulations of the agent-based model using these parameter values.
2. We decompose the parameter space of migration and proliferation probabilities $[0, 1] \times [0, 0.01]$ into a regular 11×11 grid with 121 parameter pairs (p_m, p_p) . For each parameter combination, we run n simulations of the agent-based model.
3. We calculate the cell migration rate in all simulations using the three quantification methods. The migration measurements are windowed velocities, closure rates or areas at specific time points, depending on the quantification method.
4. For each quantification method, we determine whether the migration measurements of each sampled parameter combination (p_m, p_p) are statistically significantly different from those for the focal parameter pair \hat{P} . We perform two tests: the two-sample Kolmogorov-Smirnov test and the unpaired two-sample t-test, which we refer as the K-S test and t-test, respectively. We fix a p -value < 0.05 to define statistical significance.

We consider a K-S test and a t-test to test for differences at the distribution level and in the mean. We test our data for normality and in case the migration measurements are not normally distributed, we consider a Wilcoxon rank-sum test. We account for stochasticity of the agent-based model by repeating this test for 20 times and analyse the mean and variance of the classification results.

When applying the classification test for the MEV method, we consider a global optimal window size for determining the windowed velocities of the simulations. In this way, we obtain the same number of windowed velocities for each simulation. To determine this global optimal window, we consider a weighted sum of the individual objective functions of each simulation (Supplementary Material Section S2). When applying the classification test to the area method, we must specify the time point at which the wound areas are measured and compared. We fix the comparison time to be half the time it takes the leading edges to touch each other in the first simulation, which is a common choice in an experimental setting.

2.7 Implementation

The segmentation algorithm and the data analysis are implemented in MATLAB Version: 9.3.0.713579 (R2017b). The segmentation pipeline uses functions from Matlab’s Image Processing Toolbox, the Grow Cut algorithm implementation found in <http://freesourcecode.net/matlabprojects/56832/growcut-image-segmentation-in-matlab> and the normality tests implemented by [31]. The agent-based model is implemented in NetLogo [32]. We do not apply the segmentation algorithm to the *in silico* images so the detection method does not affect the migration rate measurements.

3 Results

3.1 Exploration and validation of quantification method via *in silico* data

We first use the agent-based model to investigate how our quantification method is affected by cell migration and proliferation. Then, by applying the classification test, we investigate how well the method classifies cell populations with different migration and proliferation parameters in comparison with the other quantification methods.

3.1.1 Sensitivity analysis

We investigate how the windowed velocities are affected by the rates of cell migration and proliferation. We vary the migration and proliferation probabilities for fixed initial conditions. We decompose the parameter space of migration and proliferation probabilities $[0, 1] \times [0, 0.01]$ into a regular 11×11 grid with 121 parameter pairs (p_m, p_p) . For each parameter combination, 150 simulations were performed and the windowed velocities were calculated. The optimal window was calculated with respect to all simulations for the same parameter combination. In Figure 4 (a) we present a contour plot of the mean windowed velocity which shows how, as the probabilities increase, the mean velocity increases. A similar trend is observed for the standard deviation (see Figure 4 (b)).

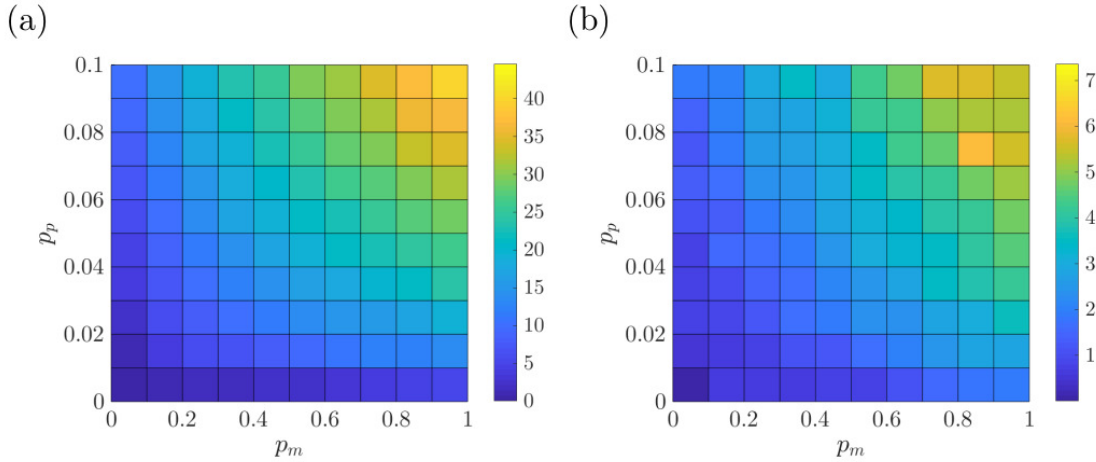


Figure 4: Sensitivity analysis of the agent-based model. We analyse the variability of the windowed velocities with respect to the proliferation and migration probabilities $(p_m, p_p) \in [0, 1] \times [0, 0.1]$. In (a) and (b), we plot the mean and the standard deviation of windowed velocities of 150 simulations under each of these 121 parameter pairs.

3.1.2 Classification performance

We suppose that the focal parameter combination, $\hat{P} = (\hat{p}_m, \hat{p}_p)$, takes values in $\{0.1, 0.5, 0.9\} \times \{0.01, 0.05, 0.09\}$ in order to test the classification for small, medium and high values of cell migration and proliferation in our

parameter space. We consider $n = 4$ simulations as the sample size for our test, so as to coincide with experimental settings in which four samples are typically used. We repeat the classification test 20 times to produce results that account for the stochasticity of the system.

In Figure 5, we plot the results of the mean behaviour of the classification tests when considering the K-S test and the three focal parameter combinations: $\hat{P} = (0.1, 0.01)$, $(0.5, 0.01)$ and $(0.9, 0.01)$. On each plot, the focal parameter combination is indicated by a red circle. At each position (p_m, p_p) , we plot a circle whose colour corresponds to the percentage of times the migration measurements of that parameter pair are statistically significantly different to those for the focal parameters \hat{P} with respect to the colourbar at the left of the plots. For parameter pairs different from the focal parameter, $(p_m, p_p) \neq \hat{P}$, the percentage of times the migration measurements of that parameter pair are statistically significantly different to those for the focal parameters \hat{P} is smaller than 100%, is an indication of the presence of false negative results. For the focal parameter, $(p_m, p_p) = \hat{P}$, if this percentage is higher than 0% then it indicates the presence of false positive results. We note that for $\hat{P} = (0.1, 0.01)$, the method does not make false negative results: the K-S test indicates that the windowed velocities from simulations of parameter pairs different from the focal parameters, $(p_m, p_p) \neq \hat{P}$, are statistically significantly different to the windowed velocities from simulations of the focal parameter pair 100% of the time (Figure 5 (a)). For $\hat{P} = (0.5, 0.01)$, there are four parameter pairs for which the velocities were 80%, 85%, 85% and 95% times statistically significantly different to those for the focal parameter (Figure 5 (b)). For $\hat{P} = (0.9, 0.01)$, the number of parameter pairs for which the percentage is not 100% increases (Figure 5 (c)). We observe that as the migration rate increases, the classification performance worsens. The intra-sample difference is accounted for when considering the classification tests for the parameter pair $(p_m, p_p) = \hat{P}$. We observe that the method gives false positive results fewer than 34 percent of the time. This percentage decreases as the proliferation probability increases (see Supplementary Material Section S3).

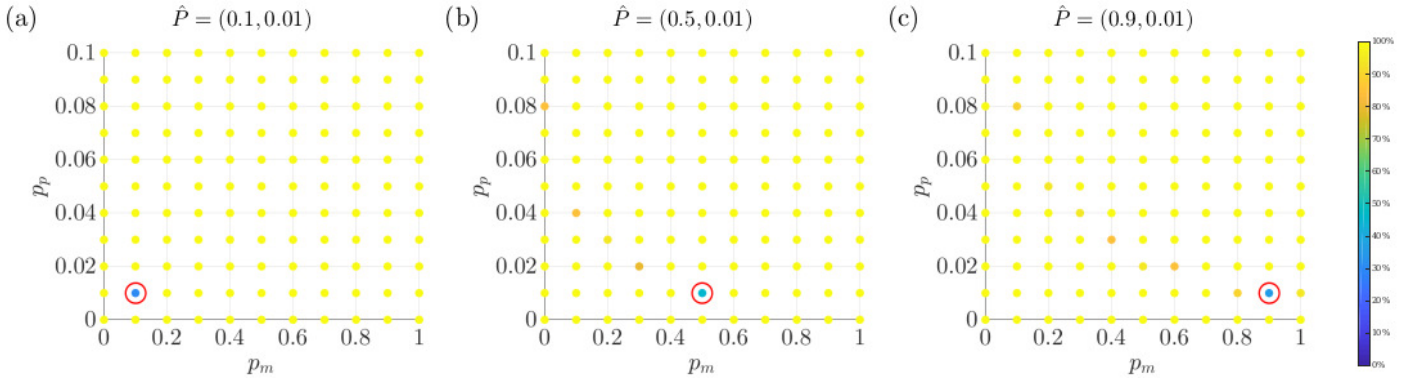


Figure 5: Plots of the mean behaviour of the classification tests for the monolayer edge velocimetry method. The classification tests are performed by considering a K-S test, a sample set of $n=4$ simulations and the focal parameters (a) $\hat{P} = (0.1, 0.01)$, (b) $\hat{P} = (0.5, 0.01)$, and (c) $\hat{P} = (0.9, 0.01)$. In each plot at each parameter pair (p_m, p_p) , the colour of the circle denotes the percentage of times the migration measurements of that parameter pair are statistically significantly different to those for the focal parameter \hat{P} . We indicate the focal parameter pair with a red circle. The plots illustrate how the classification performance of the method varies as the migration parameter varies. The method performs better when the migration parameter is small.

3.1.3 Comparison with standard migration quantification methods

We compare the classification performance of the MEV method with the closure rate and the area methods [3, 10]. As before, the focal parameter combination, \hat{P} , takes values in $\{0.1, 0.5, 0.9\} \times \{0.01, 0.05, 0.09\}$. We consider $n = 4$ simulations as the sample size and repeat the classification test 20 times.

In Figure 6, we plot the mean behaviour of the classification tests for the three quantification methods by applying the K-S test and the focal parameter combinations $\hat{P} = (0.1, 0.01)$, $(0.5, 0.01)$ and $(0.9, 0.01)$. We observe that for a focal parameter pair, the MEV method yields fewer incorrect classifications. We also observe that as the proliferation rate increases, the percentage number of incorrect classifications increases for the three methods.

The results of the classification tests for all other focal parameter combinations in $\{0.1, 0.5, 0.9\} \times \{0.01, 0.05, 0.09\}$ are presented in the Supplementary Material Section S3. Overall we observe that our method outperforms the closure rate and the area method. For all focal parameter combinations tested, the MEV method yields a greater percentage of correct classifications. The performance of the area method is the worst while the performance of the closure rate method is intermediate between our method and the area method. The performance of all three methods declines as the values of the migration and proliferation rates of the focal parameters \hat{P} increase. The optimal window sizes for each classification test are of similar size as the cell diameter (results not shown).

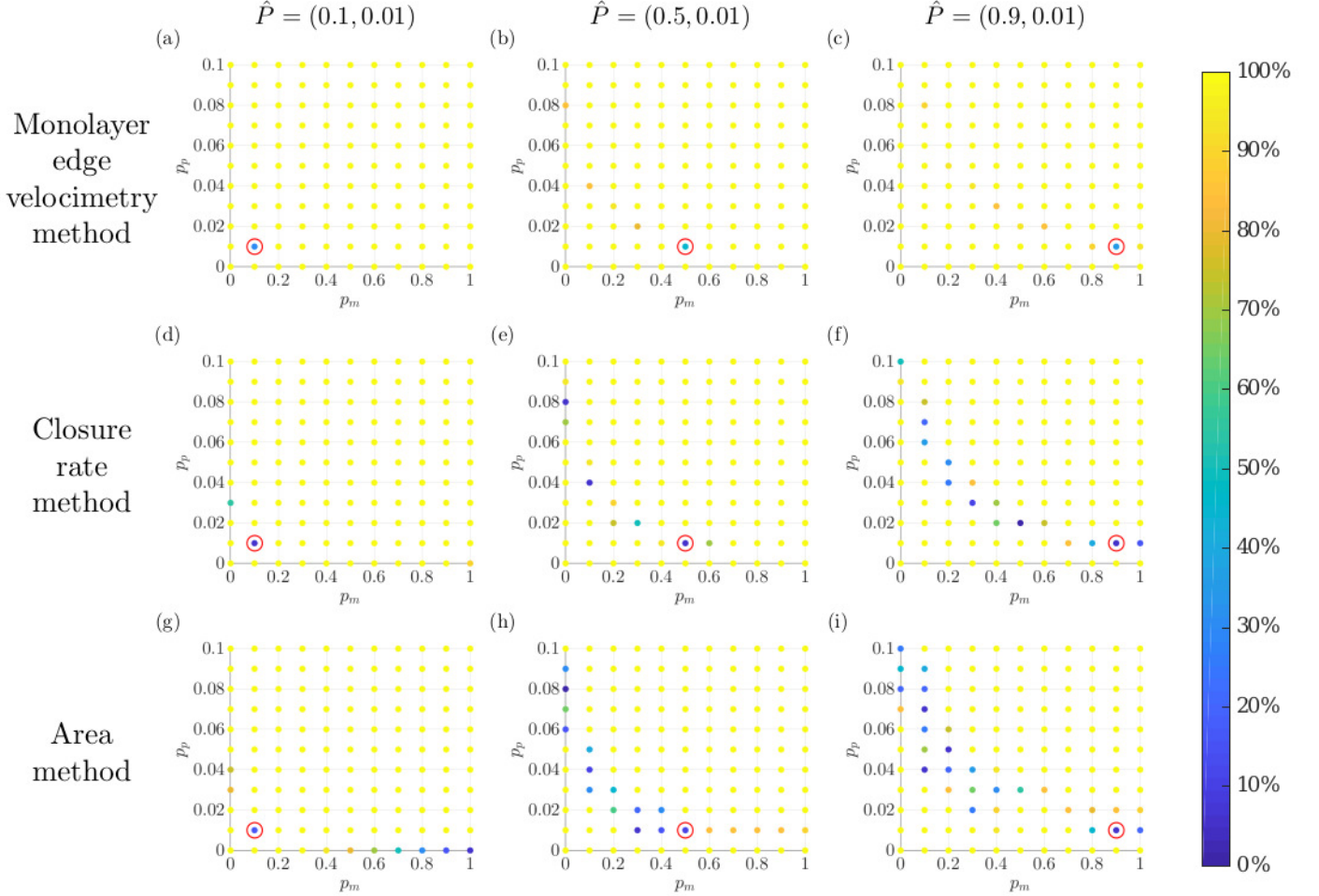


Figure 6: Series of plots showing how the performance of the three quantification methods changes as the migration rate of the focal parameters varies. In each plot, the colour of the circle at each parameter pair (p_m, p_p) indicates the percentage of times the migration measurements associated with the parameter pair are statistically significantly different from those associated with the focal parameters \hat{P} . The focal parameters \hat{P} are indicated by a red circle. The results reveal that the monolayer edge velocimetry method yields a better statistical classification than the other methods. We note also the performance of all three methods declines as the migration rate of the focal parameters \hat{P} increases.

3.2 Application of the quantification methods to in vitro data

Having tested the quantification methods on in silico data, we now use them to analyse experimental data. We first detect the position of the leading edges from the wound healing images taken during the course of the experiments. We then quantify the migration rates using the three quantification methods and analyse the statistical classification.

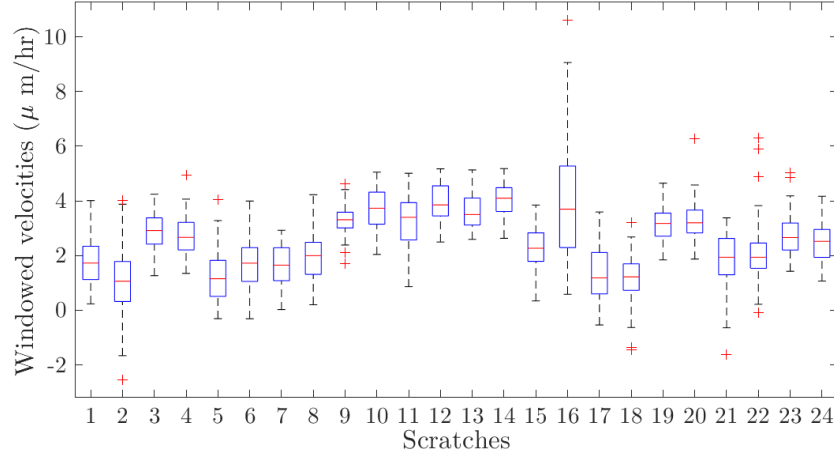


Figure 7: Boxplots of the windowed velocities with respect to the optimal window size 16 for each experimental scratch assay.

3.2.1 Image segmentation

After applying the segmentation algorithm, the front of the cell monolayer is detected for each time-lapse image. In Figure 1 we present the time-lapse data of a representative scratch from each cell group (S1-S6).

3.2.2 Quantification method results

We quantify the migration velocity of scratch assays for the different cell types using the MEV method. We determine the global optimal window by calculating the objective function for the 24 scratch assays. We vary the window size w from 1 to $500\mu m$ with a step size of $1\mu m$ and use equation (7) to calculate the objective function $F(w)$. The objective function and the three fitness functions that contribute to its calculation are shown in the Supplementary Material Section S4. The maximum value is attained for a window size of $16\mu m$. For a fixed window size ($w = 16\mu m$), we use a linear approximation to describe the position over time of the fronts and determine the 32 representative windowed velocities for each scratch assay and visualize their boxplots in Figure 7.

3.2.3 Statistical classification via the local quantification method

After grouping the velocities of scratch assays from the same cell type, the migration rate of each cell group is represented by 256 velocities. The boxplots associated with the velocity distributions for the six groups are shown in Figure 8 (a). To determine how different the migration rate of cell group S1 is from the others, we perform a K-S test to test the null hypothesis that the velocities from the two groups come from the same distribution. The null hypothesis was rejected for groups S2, S3 and S4 with statistical significance level of $p_{value} \leq 0.0001$. The null hypothesis was rejected for group S6 with statistical significance level of $p_{value} \leq 0.05$. For group S5, the null hypothesis was not rejected. We performed a t-test between S1 and each of the other groups to determine whether the mean difference is statistically significant. The mean difference between the velocities for cell groups S1 and S2, S3 and S4 is statistically significant at the 0.0001 level. There was statistical significance in the mean difference with respect to S6 at the 0.05 significance level. The statistical results for the K-S tests and t-tests are reported in Figure 8 (a). The exact value of the p_{value} for each test is reported in the Supplementary Material Section S5.

3.2.4 Statistical comparison to standard migration quantification methods

We now compare the statistical results of our quantification method against those for the area and closure rate methods. In Figure 8 (b) we plot the closure rates of each group and report the results from performing the K-S test and t-test between S1 and the other groups. S3 was the only group for which the null hypothesis of

the K-S test and the t-test was rejected at the 0.05 significance level. When we performed the statistical tests for the percentage area measurements, no significant difference was found. In Section S5 of the Supplementary Material we include the results of the K-S and t-tests for the percentage wound area measurements.

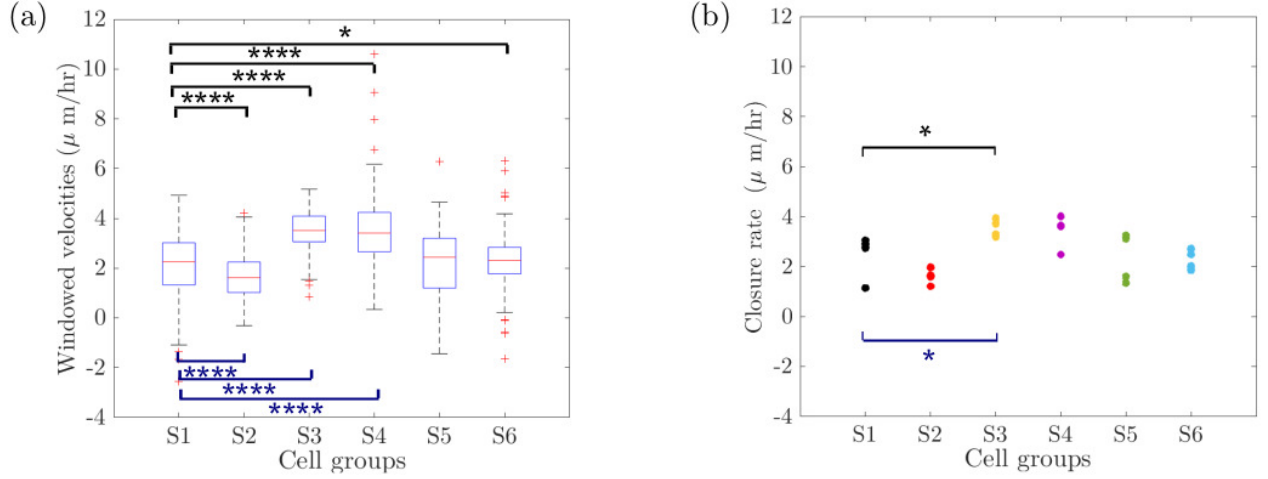


Figure 8: Statistical analysis of the experimental data using the velocity and the closure rate method. First, the migration measurements are grouped into the six different groups (S1-S6). The windowed velocities and the closure rates for the cell groups are plotted in A and B, respectively. Above the data, in black, we have reported the statistical significance results from performing a K-S test with respect to the S1 group. Below the data, we have done the same for the t-tests. Considering the windowed velocities, with respect to the K-S test and t-test, the null hypothesis was rejected testing group S1 against group S2, S3 and S4 at the 0.001 significance level. Performing the statistical tests with the closure rate measurements, the null hypothesis was rejected at the significance level of 0.05 between S1 and S3. The statistical significance level is decoded in the symbols: $*:= p_{value} \leq 0.05$, $**:= p_{value} \leq 0.01$, $***:= p_{value} \leq 0.001$ and $****:= p_{value} \leq 0.0001$.

4 Discussion and conclusions

In this work, we have introduced a new migration quantification method for scratch assays that characterizes the horizontal component of the front velocity of cell monolayers. The method involves three steps: (1) determination of an optimal window w^* with which to approximate the cell front by a function which is piecewise constant in segments of length w^* ; (2) approximation of the interface with respect to the window size w^* at each time point; and (3) linear approximation of the position over time of the interface in each of these windows. In this way we characterize cell migration in the scratch assay by the slopes of a series of linear approximations to the interface position over time in these windows. The optimal window is chosen to be the one that best fits a constant velocity profile and for which the left and right front velocities can be considered to be samples of the same distribution.

By considering an agent-based model that mimics the scratch assay, we tested the ability of our quantification method to distinguish between cell lines with known cell migration and proliferation rates. As the migration and proliferation rates increased, the mean and variance of the windowed velocities increased. This was an expected behaviour since migration and proliferation promote the interface velocity and the variance of the system increases as the migration and proliferation rates increase. By comparing our quantification method with two existing methods, we observed that our method outperforms both since it yielded a greater percentage of correct classifications than the other methods across a range of parameter values. We noticed that our method made significantly fewer statistical errors than the two other tested methods. Despite being widely used, the performance of the area method was the worst, while the performance of the closure rate method was intermediate between our method and the area method. The poor performance of the area method is due to the presence of irregular cell-free areas and to the indirect quantification of migration by a single time-point measurement. The poor performance of the closure rate method is also related to the irregularities in the data

since the closure rate method is equivalent to quantifying the migration by the slope of the linear approximation to the position of mean position of the interface over time.

After showing that our quantification method performed better on *in silico* data, we then used it to analyse our experimental data set. We calculated an optimal window of 16 μm , which is of the same order as the mean cell diameter size, and then determined the corresponding windowed horizontal velocities. By performing two sample Kolmogorov-Smirnov (K-S) and unpaired two-sample t-tests, we identified a statistically significant difference between the S1 group and groups S2-S4. The K-S test also indicated statistically significant differences with respect to group S6. We used these two tests since we wanted to detect differences at the distribution level (through the K-S test) and at the mean level (through the t-test). The closure rate method only detected statistically significant differences between S1 and S3. The closure rate data are of poor quality: more samples or better quality ones are needed to analyse the migration rate with this method. The area method was unable to detect any statistically significant differences in the dataset. Even when we tried different time points, there was no significant difference. We observed that the S1 cell group also exhibited the highest levels of expression of target genes associated with malignancy and poor prognosis, when analysed by qRT-PCR techniques (data not shown) in agreement with the detected significant differences in migration.

This study has some limitations which could be addressed in future work. For the *in vitro* experiments, the scratch was created by the removal of silicone inserts. It has been observed that the removal of silicone inserts can damage the culture surface coating and affect the cell migration rate [33]. We assume this effect is present in all cell samples so the comparative migration analysis performed by the quantification methods is not affected. Using our quantification method, we would be able to establish how the different procedures for creating the scratch affect migration rates. The statistical performance of our quantification method can be further validated on publicly available wound healing experiment data sets such as those in [34], which provide sets of assays and replicates under different experimental conditions. Currently our quantification method does not take into consideration the intra-group and inter-sample variances of the windowed velocities. In spite of that the classification performance of our quantification method is superior to the area and the closure rate method. The intra-group and inter-sample variances will be taken into consideration in the statistical assessment of the method in a future work. In this study, the agent-based model accounted solely for proliferation and migration events. Additional interactions could be included to give a more realistic description of the scratch assay and the impact of how these factors affect the quantification method could be assessed. The quantification algorithm assumes a linear approximation of the horizontal cell monolayer displacement. Our method could be adjusted to account for an initial phase during which the cells react to the presence of the wound, so the cell monolayer front position over time can be fitted to a Richards function, a non-symmetrical sigmoid function, as in [9]. Currently the method does not address image boundary effects that could potentially affect the quantification. The method could be improved to allow it to deal with the image boundary in a more precise way. One of the drawbacks of our quantification method is the uncertainty in the optimal window size since it depends on the samples. However, in our study we found that the optimal window size is of the order of the mean cell diameter and the statistical power and measurements of the quantification method are the same for window sizes of the same order (results not shown). If the mean cell diameter is known, then the optimization procedure can be omitted and the linear approximation can be performed using the mean cell diameter as the window size. The framework can also be extended to consider a time-dependent velocity field across the full monolayer, such as Cell Image Velocimetry (CIV) [15]. The challenge in this case would be to determine to which measurements we should apply statistical tests to detect significant differences in migration rates.

In summary, we have introduced a new method for migration quantification of typical scratch assay data, which can be of low quality. Many of the challenges we have overcome with our method could be avoided through improved experimental design. However, the latter would require: repeating the experiment or using more sophisticated experimental tools to create the same degree of confluence and uniform “wounds”. These are costly solutions. We note that our quantification method can be applied to the existing data. Furthermore, through the classification test based on *in silico* data, we show that even when the quality of the scratches is ideal, our quantification method is better at detecting differences in migration than the other standard methods. While generalization to other nonlinear wound models is not clear, e.g. circular model wounds, the proposed method shows that determining the velocity field along the cell front is sufficient to characterize the migration.

Data accessibility

The source code and the implementation of the algorithm as a GUI along with an example dataset and user instructions, are available at https://bitbucket.org/anavictoria-ponce/local_migration_quantification_scratch_assays/src/master/. The datasets are available in https://ganymed.math.uni-heidelberg.de/~victoria/supplementary_data_migration_quantification_scratch_assays.shtml.

Authors' contributions

TA, AM and SB designed and coordinated the study. AVPB developed the agent-based model and performed the processing and analysis of the data. SB and AVPB designed and developed the image processing pipeline. AM designed the experiments, while ES and JA performed them. HMB, PKM, TC and TA contributed to the analysis and interpretation of results. AVPB wrote the paper, on which all other authors commented and made editions. All authors gave final approval for publication.

Competing interests

The authors have no competing interests.

Funding

This work was supported by the Heidelberg Graduate School of Mathematical and Computational Methods for the Sciences [DFG grant GSC 220 in the German Universities Excellence Initiative to AVPB]; Mathematics for Industry Network [COST Action TD1409 short-term scientific missions grant to AVPB]; Consejo Nacional de Ciencia y Tecnología [411678 to JA]; Ministerio de Ciencia e Innovación [TIN2015-66951-C2-1-R and SGR 1742 to SB, SAF2017-89989-R and SAF2014-59945-R to AM]; Red de Investigación Renal REDinREN [12/0021/0013 to AM]; the CERCA Programme of the Generalitat de Catalunya to TA; Ministerio de Economía y Competitividad [MTM2015-71509-C2-1-R and MDM-2014-0445 to TA] and Agència de Gestió de Ajuts Universitaris i Recerca [2014SGR1307 to TA].

Acknowledgements

AVPB would like to thank Isabel Serra Mochales, Matthew Simpson and Andreas Spitz for helpful discussions. We would like to thank Guillem Perez for being the initial promoter of this collaboration.

Footnotes

Electronic supplementary material is available online.

References

- [1] Peter Friedl and Darren Gilmour. Collective cell migration in morphogenesis, regeneration and cancer. *Nature Reviews Molecular Cell Biology*, 10(7):445, 2009.
- [2] Li Li, Yong He, Min Zhao, and Jianxin Jiang. Collective cell migration: Implications for wound healing and cancer invasion. *Burns & Trauma*, 1(1):21, 2013.
- [3] Ayman Grada, Marta Otero-Vinas, Francisco Prieto-Castrillo, Zaidal Obagi, and Vincent Falanga. Research techniques made simple: Analysis of collective cell migration using the wound healing assay. *Journal of Investigative Dermatology*, 137(2):e11–e16, 2017.

- [4] Nina Kramer, Angelika Walzl, Christine Unger, Margit Rosner, Georg Krupitza, Markus Hengstschläger, and Helmut Dolznig. In vitro cell migration and invasion assays. *Mutation Research/Reviews in Mutation Research*, 752(1):10–24, 2013.
- [5] Chun-Chi Liang, Ann Y Park, and Jun-Lin Guan. In vitro scratch assay: a convenient and inexpensive method for analysis of cell migration in vitro. *Nature Protocols*, 2(2):329, 2007.
- [6] Kaylene J Simpson, Laura M Selfors, James Bui, Angela Reynolds, Devin Leake, Anastasia Khvorova, and Joan S Brugge. Identification of genes that regulate epithelial cell migration using an sirna screening approach. *Nature Cell Biology*, 10(9):1027, 2008.
- [7] Merlin N M Walter, Karina Therese Wright, Heidi R Fuller, Sheila M MacNeil, and William Eustace B Johnson. Mesenchymal stem cell-conditioned medium accelerates skin wound healing: An in vitro study of fibroblast and keratinocyte scratch assays. *Experimental Cell Research*, 316(7):1271–1281, 2010.
- [8] Christine Decaestecker, Olivier Debeir, Philippe Van Ham, and Robert Kiss. Can anti-migratory drugs be screened in vitro? a review of 2d and 3d assays for the quantitative analysis of cell migration. *Medicinal Research Reviews*, 27(2):149–176, 2007.
- [9] Gil Topman, Orna Sharabani-Yosef, and Amit Gefen. A standardized objective method for continuously measuring the kinematics of cultures covering a mechanically damaged site. *Medical Engineering and Physics*, 34(2):225–232, 2012.
- [10] Paola Masuzzo, Marleen Van Troys, Christophe Ampe, and Lennart Martens. Taking aim at moving targets in computational cell migration. *Trends in Cell Biology*, 26(2):88–110, 2016.
- [11] Elia Ranzato, Simona Martinotti, and Bruno Burlando. Wound healing properties of jojoba liquid wax: an in vitro study. *Journal of Ethnopharmacology*, 134(2):443–449, 2011.
- [12] Heiko Büth, Pier Luigi Buttigieg, Raluca Ostafe, Maren Rehders, Stefanie R Dannenmann, Norbert Schaschke, Hans-Jürgen Stark, Petra Boukamp, and Klaudia Brix. Cathepsin b is essential for regeneration of scratch-wounded normal human epidermal keratinocytes. *European Journal of Cell Biology*, 86(11-12):747–761, 2007.
- [13] James EN Jonkman, Judith A Cathcart, Feng Xu, Miria E Bartolini, Jennifer E Amon, Katarzyna M Stevens, and Pina Colarusso. An introduction to the wound healing assay using live-cell microscopy. *Cell Adhesion & Migration*, 8(5):440–451, 2014.
- [14] Martin Maška, Vladimír Ulman, David Svoboda, Pavel Matula, Petr Matula, Cristina Ederra, Ainhoa Urbiola, Tomás España, Subramanian Venkatesan, Deepak MW Balak, et al. A benchmark for comparison of cell tracking algorithms. *Bioinformatics*, 30(11):1609–1617, 2014.
- [15] Florian Milde, Davide Franco, Aldo Ferrari, Vartan Kurtcuoglu, Dimos Poulikakos, and Petros Koumoutsakos. Cell image velocimetry (civ): boosting the automated quantification of cell migration in wound healing assays. *Integrative Biology*, 4(11):1437–1447, 2012.
- [16] William J Ashby and Andries Zijlstra. Established and novel methods of interrogating two-dimensional cell migration. *Integrative Biology*, 4(11):1338–1350, 2012.
- [17] Wang Jin, Esha T Shah, Catherine J Penington, Scott W McCue, Lisa K Chopin, and Matthew J Simpson. Reproducibility of scratch assays is affected by the initial degree of confluence: experiments, modelling and model selection. *Journal of Theoretical Biology*, 390:136–145, 2016.
- [18] Wang Jin, Kai-Yin Lo, ShihEn Chou, Scott W. McCue, and Matthew J. Simpson. The role of initial geometry in experimental models of wound closing. *Chemical Engineering Science*, 179:221 – 226, 2018.

- [19] Catalina Ruiz-Cañada, Ángel Bernabé-García, Sergio Liarte, Carmen Luisa Insausti, Diego Angosto, José María Moraleda, Gregorio Castellanos, and Francisco José Nicolás. Amniotic membrane stimulates cell migration by modulating transforming growth factor- β signaling. *Journal of Tissue Engineering and Regenerative Medicine*, 2017.
- [20] Irina Gorshkova, Donghong He, Evgeny Berdyshev, Peter Usatuyk, Michael Burns, Satish Kalari, Yutong Zhao, Srikanth Pendyala, Joe GN Garcia, Nigel J Pyne, et al. Protein kinase c- regulates sphingosine 1-phosphate-mediated migration of human lung endothelial cells through activation of phospholipase d2, protein kinase c- ζ , and rac1. *Journal of Biological Chemistry*, 283(17):11794–11806, 2008.
- [21] Stuart T Johnston, Joshua V Ross, Benjamin J Binder, DL Sean McElwain, Parvathi Haridas, and Matthew J Simpson. Quantifying the effect of experimental design choices for in vitro scratch assays. *Journal of Theoretical Biology*, 400:19–31, 2016.
- [22] Stuart T Johnston, Matthew J Simpson, and DL Sean McElwain. How much information can be obtained from tracking the position of the leading edge in a scratch assay? *Journal of the Royal Society Interface*, 11(97):20140325, 2014.
- [23] Matthew J Simpson, Kerry A Landman, and Barry D Hughes. Cell invasion with proliferation mechanisms motivated by time-lapse data. *Physica A: Statistical Mechanics and its Applications*, 389(18):3779–3790, 2010.
- [24] Philip K Maini, DL Sean McElwain, and David I Leavesley. Traveling wave model to interpret a wound-healing cell migration assay for human peritoneal mesothelial cells. *Tissue Engineering*, 10(3-4):475–482, 2004.
- [25] Matthew J Simpson, Katrina K Treloar, Benjamin J Binder, Parvathi Haridas, Kerry J Manton, David I Leavesley, DL Sean McElwain, and Ruth E Baker. Quantifying the roles of cell motility and cell proliferation in a circular barrier assay. *Journal of the Royal Society Interface*, 10(82):20130007, 2013.
- [26] Evgeniy Khain, Mark Katakowski, Scott Hopkins, Alexandra Szalad, Xuguang Zheng, Feng Jiang, and Michael Chopp. Collective behavior of brain tumor cells: the role of hypoxia. *Physical Review E*, 83(3):031920, 2011.
- [27] Vladimir Vezhnevets and Vadim Konouchine. Growcut: Interactive multi-label nd image segmentation by cellular automata. In *proc. of Graphicon*, volume 1, pages 150–156. Citeseer, 2005.
- [28] John Canny. A computational approach to edge detection. In *Readings in Computer Vision*, pages 184–203. Elsevier, 1987.
- [29] GT Shrivakshan, C Chandrasekar, et al. A comparison of various edge detection techniques used in image processing. *IJCSI International Journal of Computer Science Issues*, 9(5):272–276, 2012.
- [30] Richard M Heiberger and Burt Holland. *Statistical analysis and data display: an intermediate course with examples in R*. Springer, 2015.
- [31] Metin Öner and İpek Deveci Kocakoç. A compilation of some popular goodness of fit tests for normal distribution: Their algorithms and matlab codes (matlab). *Journal of Modern Applied Statistical Methods*, 16(2):30, 2017.
- [32] Seth Tisue and Uri Wilensky. Netlogo: A simple environment for modeling complexity. In *International Conference on Complex Systems*, volume 21, pages 16–21. Boston, MA, 2004.
- [33] Sergio Liarte, Ángel Bernabé-García, David Armero-Barranco, and Francisco José Nicolás. Microscopy based methods for the assessment of epithelial cell migration during in vitro wound healing. *JoVE (Journal of Visualized Experiments)*, (131):e56799, 2018.
- [34] Assaf Zaritsky, Sari Natan, Doron Kaplan, Eshel Ben-Jacob, and Ilan Tsarfaty. Live time-lapse dataset of in vitro wound healing experiments. *GigaScience*, 4(1):8, 2015.